Vehicle wheel drag coefficient in relation to travelling velocity – CFD analysis

P Leśniewicz[1], **M Kulak and M Karczewski**
Institute of Turbomachinery, Lodz University of Technology, Poland

E-mail: lesniewicz.pawel@gmail.com

Abstract. In order to understand the aerodynamic losses associated with a rotating automobile wheel, a detailed characteristics of the drag coefficient in relation to the applied velocity are necessary. Single drag coefficient value is most often reported for the commercially available vehicles, much less is revealed about the influence of particular car components on the energy consumption in various driving cycles. However, detailed flow potential losses determination is desired for performance estimation. To address these needs, the numerical investigation of an isolated wheel is proposed herein.

1. Introduction

In recent years an automotive industry faced the problem of vehicle fuel consumption affected by unstable situation on the petrol market and European regulations concerning greenhouse gas emission. Problem of efficiency concerns not only cars fuelled by gasoline, but also hybrid and electric vehicles where the goal is to extend distance covered on a single battery charge. That is why the investigation of influence of different vehicle components, initially as independent, later as part of a system, on fuel or energy consumption is needed to evaluate the areas in which further improvements will be possible. Results of Euromix test cycle depicted that the leading factor is an aerodynamic drag influencing the vehicles fuel consumption by 40% [1]. This suggests that further attention should be paid to the overall vehicle aerodynamics as the key factor to diminish the energy usage (it is estimated that reduction of drag coefficient by 8% can e.g. decrease the fuel consumption by 0.2-0.3 L/100 km or increase the range of vehicle by 30-40 km).

When repartition of the overall aerodynamic drag is analysed, it can be stated that one of the significant contributions is due to the vehicle wheels, estimated at around 20% or more of the entire car aerodynamic drag [2, 3, 4]. However, a number of investigations dedicated to profound understanding of wheels' contribution to a passenger vehicle aerodynamic behaviour is still insufficient. To change this course a number of publications devoted to the topic of aerodynamics of wheels started to increase in the last decade [5, 6, 7, 8, 9, 10]. An experimental explanation of the flow phenomena created near the isolated rotating wheel in contact with the ground was firstly investigated by [11]. It is a reference point for many CFD and experimental studies conducted nowadays and, therefore, is also included herein for exactly this reason. Another experimental work on isolated wheel in a contact with the ground was done by [7, 12], who, among many tests, presented a comprehensive look on the importance of flow characteristics inside the tyre grooves in comparison to slick tyres. CFD methods were also introduced into engineering problems oriented on explaining the flow

[1] To whom any correspondence should be addressed.

intricacies of rotating wheels. One of the first CFD studies was performed by [13], to be followed by other researchers to mention only [8, 9], where studies of different numerical models were undertaken or [2] who presented an investigation of tyre deformation near the contact patch. Recent works done by [6, 14, 15] confirm that the numerical analysis of the isolated wheel as well as a wheel inside the wheel arch are indispensable part of tyre research. Today, CFD-based tyre models can predict the most important phenomena of the flow with satisfactory accuracy and are a useful tool to complement any experimental study.

Fuel consumption of a vehicle is calculated according to New European Driving Cycle (NEDC) defined by United Nations Economic Commission for Europe. NEDC cycle consists of urban (ECE 15) as well as high-speed (EUDC) parts. For an urban driving cycle test, maximum achieved speed equals 50 km/h (13.9 m/s), while for high-speed driving - 120 km/h (33.3 m/s) [16]. However, due to the increasing number of hybrid and electric vehicles the UN ECE GRPE (Working Party on Pollution and Energy) group is working on the new kind of a test, which, will complement the NEDC cycle. The new test is called Worldwide Harmonized Light Vehicles Test Procedures (WLTP) and includes three driving classes which depends on power to weight ratio. Class 3 cycle being representative of the 3rd class of the power to weight ratio will be used for currently produced vehicles. The speed range for this class is between 56 km/h (15.5 m/s) and 130 km/h (36.1 m/s) depending on the phase of the test [16]. The highway-specific phase of Cycle 3, called extra-high, has an average speed of 94 km/h (26.1 m/s). The new test thresholds, in light of the current passenger car performance, suggest that a tremendous push is required from future vehicles in order to remain competitive in the market. This will require lowering an overall energy consumption of the hybrid and all electric vehicles by smart actuation techniques, power management, but, above all, continuous reduction of energy losses, including aerodynamic drag of the wheels.

The aim of this paper is to analyse aerodynamic differences of the flow around the wheel moving with the speeds pertinent to the NEDC and WLTP test cycles, as well as to investigate the importance of wheel drag in relation to the applied velocities. This is done precisely for the purpose of the first time look at the importance of tyre designs in terms of their aerodynamic performance (energy requirement) for a range of travelling velocities observed in the aforementioned test procedures. Presented work includes numerical analysis of an isolated wheel equipped with two types of tyres - slick and tyres with longitudinal grooves. It aims at exemplifying the tendencies and similarities which could be later mapped on non-isolated cases, in order to decrease the time and computational power necessary for further research. The study includes explanation the influence of tyre tread pattern on part of the energy intake associated especially with overcoming aerodynamic resistance of all-electric vehicles in high-speed traffic. The secondary goal is to instigate discussion about importance of inspecting the aerodynamic resistance of wheels in the function of various travel velocities. Such characteristics could find use in future smart actuation systems responsible for energy distribution in all electric vehicles.

2. Model description and validation

The above research aims at establishing a set of guidelines for flow around wheel simulation, proposing the approach with investigation of isolated wheel only (without necessity of including car body to the virtual model). Observing the presence of phenomena and differences resulting from geometrical features e.g. wheel tread, existing in both cases, one can significantly decrease the cost and time of computation by research of isolated wheel.

Mlinaric [2] has given a broad look at computational methods of simulating flow around a vehicle wheel as based on passenger cars manufactured by Volvo Car Corp. His work describes the importance of utilising a more robust technique of simulating the motion of vehicle wheels. It was decided to use MRF technique in simulations presented in the following paper, mainly to limit the computational time and resources needed to perform a vast number of computations for the analysed travel velocities.

The investigated wheel geometry was based on the tyre analysed by [11]. Diameter of the wheel was equal to 416 mm, while the breadth was 191 mm. The same tyre with three longitudinal grooves evenly distributed with respect to the wheel's centreline was used to study the effect of tread geometry. Dimensions of the grooves are as follows: 6.35 mm wide and 3.175 mm deep. In order to obtain good relation between mesh elements amount and accuracy of the results, comparison of the drag coefficient and mesh size was done for both types of tyres. Independence of drag values was investigated by changing size of the elements and calculating drag values for different mesh sizes. Computationally solid results were observed for the meshes with number of elements around 6 mln for slick tyre, and 13 mln for a tyre with grooves (for more details see [14]). SST turbulence model was applied as the best compromise between accuracy of the results and time needed for simulation. This model was previously validated for tyre studies [6, 14], and benchmarked for the modelling of aerodynamic flow phenomena induced by rotating machine elements [17]. Flow was treated as isothermal and fully turbulent with air as ideal fluid at temperature equal to 25°C. Spatial discretization of governing equations along with turbulence closure was second order accurate. Boundary conditions applied to the model are presented in Fig. 1. Opening boundary condition indicates that the fluid can freely move in and out of the domain. Tyre surfaces were defined to be smooth with no slip boundary conditions applied. At the inlet, uniform flow velocity condition was applied with turbulence intensity of 0.2%. The ground was modelled as no slip wall with wall velocity equal to travel velocity. At the outlet, average static pressure with relative pressure equal to 1 atm and pressure profile blend 0.05 was applied. To enable analysis of tyre aerodynamics at various travel velocities, the free stream flow speed was changed depending on the analysed case. All other simulation parameters were then held constant. Because the analysed speed range expands considerably, the Reynolds number effects on flow behaviour have to be considered. For this reason, the numerical model at lower and upper ranges of analysed velocities was validated against available experimental data. The details regarding the validation at low speed conditions can be accessed in [14]. The validation at the upper range of the considered driving cycles is presented below.

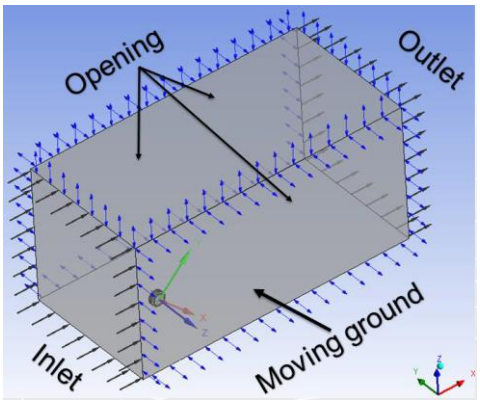

Figure 1. Boundary conditions.

In light of the absence of experimental tests performed at velocities in the upper portion of the NEDC and WLTP tests (33-36 m/s), the results from experimental campaign by [7] were used, where aerodynamic performance of tyre with 4 grooves was assessed at 40 m/s for a generic isolated racing car tyre positioned at 2° camber angle.

Results of the experimental investigation presented in [7] were converted form force values to drag and lift coefficients. Table 1 presents results of Cx - drag and Cz -lift coefficients obtained from experimental work, CFD done by [18] and own numerical simulations.

Table 1. Results of experimental investigation in relation to the CFD simulations in terms of lift and drag coefficients obtained for the upper velocity range of analysed driving cycles.

Parameter	Experiment [7]	CFD [18]	Own CFD
Drag coeff. (Cx)	0.444	0.590	0.482
Lift coeff. (Cz)	0.058	0.235	0.244
% Difference Cx	-	32.8	8.6

Such low value for experimental Cz was caused by the lack of tyre deformation in the contact area due to the materials that were used to make the wheel model (aluminium and composite materials). The wheel was slightly elevated above the belt used to simulate the moving ground condition. That caused the pressures to equalise what was manifested in the unusually small lift force. On the other hand, the drag coefficient is likely to be slightly higher shall the wheel camber be reduced to 0°. At the same time, own simulation results for the tyre with grooves produced Cx = 0.487 and Cz = 0.252 at V = 41.7 m/s. Although a number of grooves is different in own study (herein 3 grooves) from the model in [7] (4 grooves), the obtained result of Cx shows signs of convergence with the work presented by [7]. As the objective of the above article is to identify general tendencies in drag – velocity relations, the level of similarities between both models was considered as acceptable for the purpose of initial comparison. Presented research is aiming at in-house experiment covering both isolated and non-isolated wheel supported with corresponding CFD simulations. The same group of researchers in [18] also performed numerical study applying the identical boundary conditions as in own experiment [7]. Differences between drag values for the experimental and numerical work in [18] were explained by "slightly higher pressures behind the wheel" in case of the experiment which led to the smaller drag force. Comparing results of this investigation with the experimental data presented in [18] it can be observed that, own model is closer to the presented work and can be considered as representative for the upper range of the analysed velocities.

3. Results and discussion

3.1. Drag and lift

In the following section results of the numerical simulations made using ANSYS CFX ver.14 will be included. Speed ranges were selected based on the NEDC and WLTP tests described in the introduction section and vary from 13.1 m/s up to 36.1 m/s. Detailed description of applied velocities, equivalent Reynolds number (Re) together with values of global quantities such as drag (Cx) and lift (Cz) coefficients are presented in Table 2.

Table 2. Results of lift and drag coefficients of isolated slick and grooved wheel model, results derived from own CFD simulations.

V [m/s]	Re [-]	Cz [-] slick	Cz [-] grooved	Cx [-] slick	Cx [-] grooved	ΔCx (with respect to slick)
13.1	3.48E+05	0.287	0.234	0.541	0.528	-0.013
15.8	4.19E+05	0.293	0.239	0.538	0.521	-0.017
18.6	4.93E+05	0.295	0.261	0.535	0.520	-0.015
21.4	5.68E+05	0.294	0.277	0.532	0.520	-0.012
24.2	6.42E+05	0.292	0.279	0.530	0.520	-0.010
26.9	7.14E+05	0.289	0.274	0.526	0.517	-0.009
30.6	8.11E+05	0.288	0.271	0.520	0.508	-0.012
33.3	8.84E+05	0.288	0.264	0.514	0.502	-0.012
36.1	9.58E+05	0.288	0.256	0.509	0.492	-0.017
38.8	1.03E+06	0.290	0.253	0.510	0.486	-0.024
41.7	1.11E+06	0.288	0.252	0.505	0.487	-0.018

What is more, ΔCx which shows differences in drag values between the slick tyre and the tyre with grooves was also estimated. This drag delta is quite consistent also in the experimental and numerical tests of a passenger vehicle model as it was presented in [6]. Analysing relation between the drag versus applied velocities presented in Fig. 2 as well as in the table above, it can be observed that Cx decreases while the speed is increasing. This phenomenon occurs in case of slick and grooved tyres. Results allow to state that the grooves lower the aerodynamic drag independently from velocity applied. The difference in aerodynamics-based energy loss is nearly constant when both characteristics are compared. Many phenomena will be better clarified when planned own experiments for the studied wheel models at a reduced scale will be performed in the wind tunnel facility using PIV (Particle Image Velocimetry) to visualize flow structures. To the authors' best knowledge, such extended analysis, be it numerical or experimental have not been conducted.

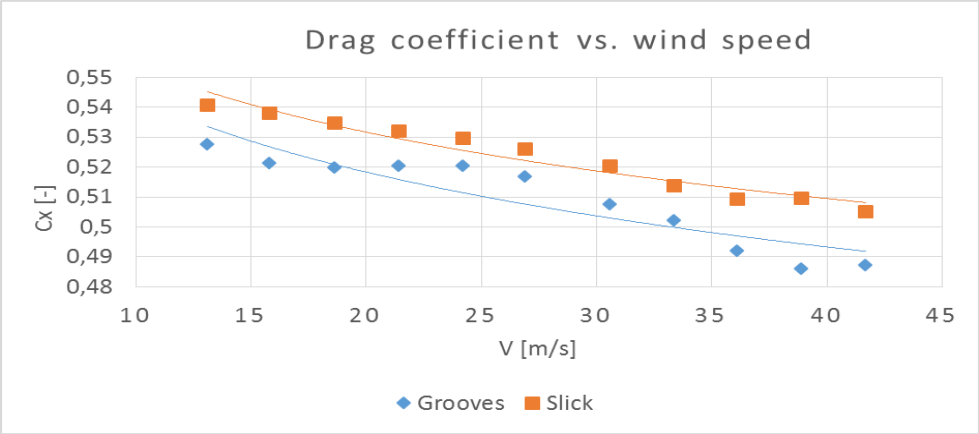

Figure 2. Characteristics of an isolated slick and grooved wheel's drag coefficient in relation to the travel velocities found in European driving test cycles

3.2. Estimation of the energy needed to overcome the aerodynamic drag of the wheels

Using travel velocity data of the analysed driving test cycles it is possible to estimate the energy usage needed to overcome the aerodynamic drag of the wheels. Table 3 includes information about purely aerodynamic-based average energy needed for 4 wheels, with and without the grooves, to cover the distance used in WLTP and EUDC test procedures. All input data were taken from [16]. Calculation procedure was based on power determination achieved by multiplication of the velocity and aerodynamic drag force in the travel direction. What is more, times needed to cover the distances mentioned in the test procedures were included into calculations to obtain relevant required power. Results were presented in the form of watt-hour as a unit of energy.

Table 3. Average energy consumption associated with aerodynamic losses of the analysed vehicle wheel types estimated as based on three European driving cycles.

Tyre type	High part of WLTP (16.9 m/s)	Extra high part of WLTP (26.1 m/s)	EUDC part of NEDC (19.3 m/s)
Slick tyres [Wh]	82	171	72
Tyres with grooves [Wh]	81	169	71
Δ%	1.2	1.2	1.4

It can be observed that more energy is needed to overcome the aerodynamic drag of the slick tyre what is connected with the drag difference observed on the earlier plot. For a drive with the average velocity of 90 km/h (extra high part of WLTP) this difference is twice as big as for the high part of the same cycle. This is especially meaningful at much longer distances and higher velocities (even up to

130 km/h) that are being covered during a motorway traffic. When analysing differences between wheels having slick and grooved tyres, it can be observed that only by changing the shape of the tread (adding three longitudinal grooves) it is possible to reduce the energy usage by 1.2 % up to 1.4 %.

3.3. Pressure distribution

The pressure distribution on a wheel's surface is being presented in the form of 3D visualization. Figures 3 and 4 show pressure coefficient Cp distributions from the bottom (contact region side, air flow from left to right in order to preserve the same direction in the simulations and the experimental work) and the upstream view perspectives. Results of own numerical investigations for tyre with grooves were compared to the experimental study [7]. Slightly different geometry was investigated by Dimitriou et al., where four grooves were used, and the wheel was positioned at the 2° wheel camber. What is more, during the experiment, the model was equipped with outriggers to hold it, what could have potentially caused additional flow differences.

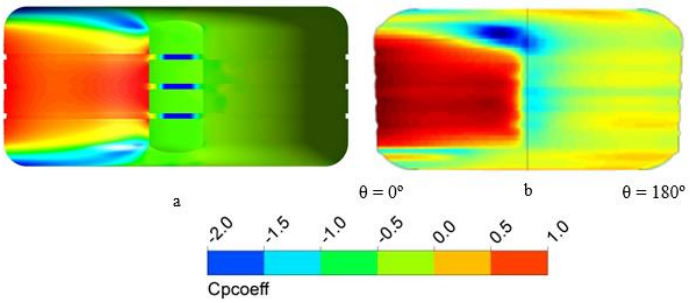

Figure 3. Bottom view of Cp pressure distribution for the tyre with the grooves – CFD investigation with velocity 36.1 m/s (a) and experiment made by [7] at 40 m/s (b)

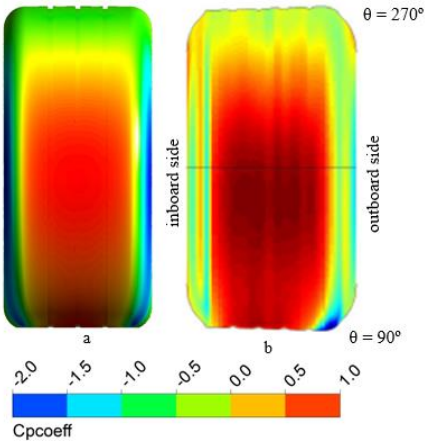

Figure 4. Upstream view of Cp pressure distribution for the tyre with the grooves – CFD investigation with velocity 36.1 m/s (a) and experiment made by [7] at 40 m/s (b)

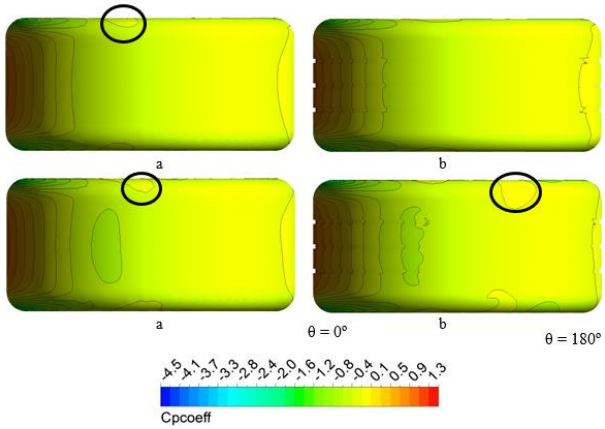

Figure 5. Top view of Cp pressure distributions for the slick tyre (a) and tyre with grooves (b) at velocities of 13.1 m/s (upper row) and of 36.1 m/s (bottom row)

Nevertheless, the upstream view of the pressure distribution shows similarities between numerical and experimental investigations around the stagnation region (θ angle equal to 0º), where the highest values of pressure can be observed. Pressure increase can be noticed in the middle part of the tyre surface, while close to the sides the decrease of pressure can be observed. The distribution differs between numerical and experimental results especially in the upper part of the visible wheel section. Boundary layer is formed from a stagnation point (θ = 0°) and separates behind the top of the wheel (around θ = 270°). The decrease of static pressure in the separation region leads to the acceleration of

the stream. The small wheel camber used for the model tested experimentally causes asymmetric pressure distribution. At the outboard side the pressure drop associated with the jetting is also present in the CFD simulation. On the inboard side this is no longer true as applying camber diminishes the contact patch size and tends to equalize the pressures (Cp value is likely to approach 0 while wheel camber increases), what is visible in case of the wheel on the imprint 4b. With camber equal to 0° in the simulations, distribution remains symmetric there. In Fig. 3b it can be further observed that the small camber angle causes the pressure distribution around the wheel to be no longer symmetric. Additional discrepancies may be connected with experimental stand configuration in which the contact between wheel and the ground was not fully developed. Hence the pressure drop visible in the three grooves (Cp around -2.0) finds no similarities in the experimental results. In case of the experimental work, the decrease of pressure was also observed, however its intensity was much smaller (Cp around -1.0) due to the under-developed contact patch - wheel model made form aluminium and composite materials was unloaded and had to be kept at a certain minimal distance away from the moving ground belt. However, for the major part, pressure distributions in the centre part of the wheel from the stagnation point towards the contact region ($\theta = 0^o$ to 90^o) look very similar (CFD vs. experiment). In both cases increased value of pressure is observed. Apart from the exact value of pressure coefficient in the contact region, both models show pressure decrease in that area as well as Cp increase behind the contact patch.

In order to analyse the pressure differences on the wheel surface between slick tyre and tyre with grooves in relation to the minimum and maximum velocity applied, it was decided to further compare the distribution of pressure at the top surface of the wheel. Figure 5 presents top views of pressure distribution. In the upper part of the figure results of simulations with velocity 13.1 m/s are presented, while in the bottom part those with V = 36.1 m/s. The pressure drop after passing the $\theta = 270°$ angle is more severe for the higher values of velocity. In case of the slick tyre pressure drop near the separation region shows more regular shape than for the tyre with grooves what is connected to the fact that some portion of the air travels through the grooves. The second difference is related with the sides of the tyre (inboard and outboard). In case of the slick tyre, the pressure increase can be observed on the side of the wheel, the only difference was connected with the size which in case of higher velocity was larger (region marked in black). When comparing tyre with grooves it can be observed that for velocity equal to 13.1 m/s such a pressure increase was not observed. Results of simulation with higher velocity show increase of pressure near to the side of the wheel. Its structure and location differs in relation to the slick tyre. In this case higher pressure region is moved to the lower value of theta angle and its influence on the tread part of the tyre is more significant.

4. Conclusions

Numerical investigation was carried out to characterise the relation between Reynolds number and the value of drag for isolated rotating wheel equipped with slick tyre and tyre with three longitudinal grooves. Presented model was verified based on the experiments performed by [7,11,12]. CFD analysis showed flow characteristic for different velocities applied to the model. Relation between drag, lift coefficients and pressure force was also presented. Differences in pressure distribution between analysed cases were identified and explained in relation to the experimental studies. Due to the obtained characteristics, attention was also paid to the velocity distribution at the top of the wheel ($\theta = 270^o$). What is more, estimation of the energy usage needed to overcome the aerodynamic drag of the wheels was presented to shed the light on the energy management in terms of electric vehicle. Presented calculation may be a useful step for the introduction of the new category in the tyre labelling regulations related to the energy needed to overcome the tyre's aerodynamic resistance. Above work is only the first step in discussion about new tyre labelling categories in which significant contribution will be connected with the WLTP driving cycle and the new vehicle class division based on power to weight ratio. Tyre manufacturers may be forced to add new categories to the labelling system, not only in relation to aerodynamic resistance, but also to aquaplaning or driving stability. Nowadays customers' needs are the key factors in automotive industry and authors expect that in the near future

car buyers would like to know how individual car parts (such as wheels and tyres) over which they hold the purchasing power help them save energy and extend the distance covered on a single battery charge. That is why, it is high time to open the discussion about methods and procedures of additional tests useful in establishing new labelling categories for the tyres.
The second main point is related to the creation of first aerodynamic characteristic of the wheel (equipped with slick tyre and tyre with grooves) in the wide range of the velocities. Such a characteristics performed on the experimental stand surely constitute a very important contribution to the development of the energy distribution control algorithms. It is planned to support the numerical investigations with in-house experiment, focusing on isolated as well as non-isolated wheel. Developed methodology, while verified by wind tunnel tests, could be applicable both to scientific researches and to industrial purposes.

References

[1] Piechna J 2000 Podstawy aerodynamiki pojazdów WKŁ Warszawa
[2] Mlinaric P 2007 Investigation of the influence of tyre deformation and tyre contact patch on CFD predictions of aerodynamic forces on a passenger car (Chalmers University of Technology)
[3] Regert T and Lajos T 2007 Description of flow field in the wheelhouse of cars *Int. J. of Heat and Fluid Flow* **28** 616-629
[4] Croner M, Bezard H, Sicot C and Mothay G 2013 Aerodynamic characterization of the wake of an isolated rolling wheel *Int. J. of Heat and Fluid Flow* **43** 233-242
[5] Diasinos S 2009 The Aerodynamic interaction of a rotating wheel and a downforce producing wing in ground effect (University of New South Wales)
[6] Kulak M, Karczewski M and Spolaore G 2014 Flow around rotating wheels and its interaction with vehicle aerodynamics – CFD vs. wind tunnel tests *FISITA world congress* (Maastricht) F2014-LWS-068
[7] Dimitriou I and Klussmann S 2006 Aerodynamic forces of exposed and enclosed rotating wheels as an example of the synergy in the development of racing and passenger cars *SAE Int.* **2006-01-0805**
[8] McManus J and Zhang X 2006 A Computational study of the flow around an isolated wheel in contact with the ground *J. of Fluids Eng.* **128** 520-530
[9] Ramachandran D and Doig G C 2012 Unsteady flow around an exposed rotating wheel (University of New South Wales)
[10] Landstrom C, Josefsson L, Walker T and Lofdahl L 2012 Aerodynamic effects of different tire models on a sedan type passenger car *SAE Int. J. Passeng. Cars - Mech. Syst.* **5** 136-151
[11] Fackrell J E 1974 The Aerodynamics of an isolated wheel rotating in contact with the ground (Imperial College London University of London)
[12] Mears A P, Dominy R G and Sims-Williams D B 2002 The Air flow about an exposed racing wheel *SAE Int.* **2002-01-3290**
[13] Axon L, Garry K and Howell J 1999 The Influence of ground condition on the flow around a wheel located within a wheelhouse cavity *SAE Int.* **1999-01-0806**
[14] Lesniewicz P, Kulak M and Karczewski M 2014 Aerodynamic analysis of an isolated vehicle wheel J. of Physics: Conf. Series **530** 012064
[15] Hobeika T, Sebben S and Landstrom C 2013 Investigation of the influence of tyre geometry on the aerodynamics of passenger cars *SAE Int.* **2013-01-0955**
[16] https://www.dieselnet.com/standards/cycles
[17] Lipian M, Karczewski M and Olasek K 2015 Sensitivity study of diffuser angle and brim height parameters for the design of 3 kW diffuser augmented wind turbine *Open Engineering* **5.1**
[18] Hashmi A A and Dimitriou I 2006 Needs & possibilities for the correction of drag and lift wheel forces which have been derived by integrating its static pressure distribution *SAE Int.* **2006-01-3623**